TM - 1073
1503.000

$\bar{P}$ Bunch RF Rotation in the Debuncher Ring with a Very Small η ($= \frac{1}{\gamma_T^2} - \frac{1}{\gamma_0^2}$)

----Effect of Higher Order Terms in Momentum Compaction Factor $\alpha_p(\Delta P/P_o)$ and Its Correction----------

Ainosuke Ando and Ken Takayama

October 1981

Fermi National Accelerator Laboratory, Batavia, IL 60510, USA

$\bar{P}$ Bunch RF Rotation in the Debuncher Ring with a Very Small η ($= \frac{1}{\gamma_T^2} - \frac{1}{\gamma_0^2}$) ----Effect of Higher Order Terms in Momentum Compaction Factor $\alpha_p(\Delta P/P_o)$ and Its Correction----------

Ainosuke Ando and Ken Takayama

October 1981

Fermi National Accelerator Laboratory, Batavia, Il 60510, USA

Contents

Abstract

Synchrotron Oscillation in accelerators or storage-rings with a very small η ($= \frac{1}{\gamma_T^2} - \frac{1}{\gamma_0^2}$) can not be regarded as the ordinary pendulum oscillation. But, by the correction of lattice parameters, it is possible to minimize differences from the normal synchrotron oscillation.

1. Introduction

A scheme/1/ has been recently proposed to produce a high-intensity antiproton beam in a stochastic cooling accumulator. According to this scheme the $\overline{P}$ beam from a $\overline{P}$ target, parameters of which are shown in Table 1, is injected in one turn in the Debuncher Ring. Each $\overline{P}$ bunch is captured by a stationary bucket. After the momentum spread of 4% is reduced by some RF manipulations, the beam is transferred to the Accumulator Ring.

From requirements of beam transfer from the Debuncher to Accumulator and stochastic cooling accumulation, as small a final debunched momentum spread as possible is desired. For this purpose , the method of the so-called RF rotation/2/ is used. In this RF manipulation, the Debuncher Ring with the small value of η ($=\frac{1}{\gamma_T^2}-\frac{1}{\gamma_0^2}$) is designed from requirements of possible RF voltage.

Although we neglect the non-linearity coming from the RF bucket, the synchrotron oscillation in such a ring can not be approximated in the term of the linear phase rotation. Namely the non-linearity coming from kinematical terms which couple with lattice parameters may become significants.

In the present paper we study in detail the effects of the above non-linearity on the $\overline{P}$ bunch which has completed RF rotation. In addition, we explain a systematic correction method of lattice parameters to minimize its effects.

Table 1

Total Energy of $\bar{P}$	8.93826 GeV
No. of $\bar{P}$ Bunches/Cycle	82
No. of $\bar{P}$/Bunch	$1.22*10^6$
Total No. of $\bar{P}$/Cycle	10^8
Bunch Length (4σ)	$\pm$12.8cm($\pm$8.21°)
$\Delta P/P_o$ (uniform distribution	$\pm$2 %
Transvers Emittance (Ex=Ey)	20 mm mrad
Cycle Time	2 sec

2. Longitudinal Motion of $\bar{P}$

2-a Recursion Equations for Synchronous Oscillation

The theory of longitudinal phase motion, describing the energy and phase oscillations that occur when a particle passes repitively through one or more " accelerating cavities " situated at localized points around the accelerator ring, is well known. Since the oscillations normally are at a relatively low frequency, it is often legitimate as well as convenient to analyze them theoretically with differential equations derived by spreading the accelerating field uniformaly around the orbit. In reality the energy changes experienced by a particle are better represented by step equations and depend on the sine of the electrical phase angle ϕ at which the particle traverses the cavity. The corresponding equations of motion are therefore non-linear and discrete.

We consider here the case of stationary motion. To obtain the actual transformation, we consider a short RF cavity system operating at a harmonic number h and an angular frequency ω_{rf}. The quantities denoted by E_n and ϕ_n are, respectively, the energy and the electrical phase angle with which a particle enters the cavity at the time of transit. Then the non-linear transformation may be written as follows:

$$E_{n+1} = E_n + eV\sin\phi_n \tag{1-1}$$

$$\phi_{n+1} = \phi_n + \omega_{rf}\cdot\frac{2\pi}{\omega(E_{n+1})} \tag{1-2}$$

where $eV\sin\phi_n$ is the energy gain per turn and the revolution period $2\pi/\omega(E_{n+1})$ is described in the form

$$\frac{2\pi}{\omega(E_{n+1})} = \frac{C_0\left(1+\alpha_p\cdot\frac{\Delta P}{P_0}\right)}{c\left[1-(m_0c^2/E_{n+1})^2\right]^{1/2}} \tag{2}$$

with C_0---the length of the closed orbit corresponding to the synchronous energy E_0,

c ---the light velocity,

m_0c^2---the rest mass of $\overline{P}$,

E_{n+1}---the energy of a particle at the (n+1)-th transit,

$\Delta P/P_0$---the momentum deviation from the synchronous momentum P_0 $(E_{n+1}-E_0)/\beta_0^2E_0$,

α_p---the momentum compaction factor.

The synchronous particle is defined by the equation

$$\omega_{rf} = h\cdot\omega(E_0).$$

Now α_p may be written in the form

$$\alpha_p = \alpha^{(0)} + \alpha^{(1)} \cdot \left(\frac{\Delta P}{P_0}\right) + \alpha^{(2)} \left(\frac{\Delta P}{P_0}\right)^2 + O\left(\left(\frac{\Delta P}{P_0}\right)^3\right), \quad (3)$$

where $O((\Delta P/P_0)^3)$ is the Landau symbol. In the present study, we neglect higher order terms than the second order one, since we suppose that these terms are small compared with other lower order terms. Evidently the momentum compaction factor α_p depends on linear lattice's parameters and the chromaticity correction system. In particular $\alpha^{(0)}$ is decided exactly from requirement of

$$\eta = \frac{1}{\gamma_T^2} - \frac{1}{\gamma_0^2} \quad , \text{ or } \quad \alpha^{(0)} - \frac{1}{\gamma_0^2}$$

where γ_T is the so-called transition gamma. On the other hand we do not know the exact value of $\alpha^{(1)}$ at this stage. Therefore we cosider the cases with the fixed $\alpha^{(0)}$ and various $\alpha^{(1)}$ in this section. However it is noted that an usual machine roughly has coefficients $\alpha^{(0)}$, $\alpha^{(1)}$ of same order.

2-b Phase Space Structure

We study the phase space structure of the system which is described in the form of recursion Eqs.(1-1),(1-2). To do so, the ordinary mapping method is taken which is useful for studying a complicated non-linear system. Then the RF parameters and other parameters which are chosen in numerical computations are listed in Table 2.

Table 2

Coefficients of Momentum Compaction Factor

$\alpha^{(0)}$		1.3018×10^{-2}
$\alpha^{(1)}$		$-4.\sim+4.\times10^{-2}$
$\alpha^{(2)}$		0.
γ_0	E_0/m_0c^2	9.486
γ_T	$1/\sqrt{\alpha^{(0)}}$	8.765
η	$1/\gamma_T^2 - 1/\gamma_0^2$	0.002
Harmonic	h	90
RF Voltage	V	2. MV
Average Machine Radius	R	80.4 m

Each of Fig. 1-a$\sim$1-i shows the phase spase structure of the system with the different $\alpha^{(1)}$. We can see the remarkably modified RF bucket and the existance of two stable resonance regions, particularly in Fig.1-a$\sim$1-d. They also indicate the sensitivity of the phase space structure to the parameter $\alpha^{(1)}$. So we make the reason clear why such a non-linearity appears in the above system , on the basis of the approximate Hamiltonian.

First of all we may expand the right hand side of Eq.(2) in $\Delta P/P_0$

$$\frac{2\pi}{\omega(E_{n+1})} = \frac{2\pi}{\omega_0}\left[1 + \eta\cdot\frac{\Delta P}{P_0} + \left(\alpha^{(1)} - \frac{\eta}{\gamma_0^2} + \frac{3\beta_0^2}{2\gamma_0^2}\right)\left(\frac{\Delta P}{P_0}\right)^2 + \left\{\alpha^{(2)} - \frac{2\beta_0^2}{\gamma_0^2} - \frac{\alpha^{(1)}}{\gamma_0^2} + \frac{\eta}{\gamma_0^4} + \frac{\beta_0^2}{2\gamma_0^2}\left(3\alpha^{(0)} - \frac{5}{\gamma_0^2}\right)\right\}\left(\frac{\Delta P}{P_0}\right)^3 + O\left(\left(\frac{\Delta P}{P_0}\right)^4\right)\right], \quad (4)$$

with $\eta = \alpha^{(0)} - 1/\gamma_0^2$,

$\frac{\Delta P}{P_0} = (E_{n+1} - E_0)/\beta_0^2 E_0$.

From Eq.(4) we obtain ϕ_{n+1} in the form

$$\phi_{n+1} = \phi_n + h\cdot 2\pi\Big[\ \eta\cdot\Big(\frac{\Delta P}{P_0}\Big) + \Big(\alpha^{(1)} - \frac{\eta}{\gamma_0^2} + \frac{3\beta_0^2}{2\gamma_0^2}\Big)\Big(\frac{\Delta P}{P_0}\Big)^2 + \Big\{\alpha^{(2)} - \frac{2\beta_0^2}{\gamma_0^2} - \frac{\alpha^{(1)}}{\gamma_0^2} + \frac{\eta}{\gamma_0^4} + \frac{\beta_0^2}{2\gamma_0^2}\Big(3\alpha^{(0)} - \frac{5}{\gamma_0^2}\Big)\Big\}\Big(\frac{\Delta P}{P_0}\Big)^3 + O\Big(\Big(\frac{\Delta P}{P_0}\Big)^4\Big)\Big]. \tag{5}$$

Futher, replacing $\Delta P/P_0$ with δ_{n+1}, we have the non-linear recursion equations which take the form

$$\delta_{n+1} = \delta_n + \frac{eV}{\beta_0^2 E_0}\sin\phi_n, \tag{6-1}$$

$$\phi_{n+1} = \phi_n + 2\pi h\cdot\big[\ \eta^{(0)}\delta_{n+1} + \eta^{(1)}\delta_{n+1}^2 + \eta^{(2)}\delta_{n+1}^3 + \cdots\big], \tag{6-2}$$

with

$$\eta^{(0)} = \eta,$$

$$\eta^{(1)} = \alpha^{(1)} - \frac{\eta}{\gamma_0^2} + \frac{3\beta_0^2}{2\gamma_0^2} \doteqdot \alpha^{(1)} + \frac{3\beta_0^2}{2\gamma_0^2}, \tag{7}$$

$$\eta^{(2)} = \alpha^{(2)} - \frac{2\beta_0^2}{\gamma_0^2} - \frac{\alpha^{(1)}}{\gamma_0^2} + \frac{\eta}{\gamma_0^4} + \frac{\beta_0^2}{2\gamma_0^2}\Big(3\alpha^{(0)} - \frac{5}{\gamma_0^2}\Big) \doteqdot \alpha^{(2)} - \frac{2\beta_0^2}{\gamma_0^2}, \tag{8}$$

.

.

.

From (6-1),(6-2), we approximate the system to the Hamiltonian which is described in the terms

$$H(\phi,\delta;t) = \frac{2\pi h}{T_0}\Big[\frac{\eta^{(0)}}{2}\delta^2 + \frac{\eta^{(1)}}{3}\delta^3 + \frac{\eta^{(2)}}{4}\delta^4 + \cdots\Big] + \frac{eV}{T_0\beta_0^2 E_0}\cos\phi, \tag{9}$$

where T_0 is the rotation period of the synchronous particle with the energy E_0. Next changing the time scale

$$t' = \frac{2\pi h}{T_0}t,$$

we have the Hamiltonian

$$H'(\phi,\delta;t') = \frac{\eta^{(0)}}{2}\delta^2 + \frac{\eta^{(1)}}{3}\delta^3 + \frac{\eta^{(2)}}{4}\delta^4 + \cdots\cdots + \lambda\cos\phi, \tag{10}$$

with

$$\lambda = \frac{eV}{2\pi h\beta_0^2 E_0}.$$

If we restrict ourselves to the region of $|\delta| \leqq \pm 5 \times 10^{-2}$, we can neglect higher order terms than the third order term because of

$$\frac{\eta^{(2)}}{4}\delta^4 \quad \gg \quad \text{higher order terms}$$

Hence the Hamiltonian (8) becomes

$$K(\phi, \delta ; t') = \frac{\eta^{(0)}}{2}\cdot\delta^2 + \frac{\eta^{(1)}}{3}\cdot\delta^3 + \frac{\eta^{(2)}}{4}\delta^4 + \lambda\cos\phi \qquad (11)$$

The canonical equations derived from (11) are

$$\frac{d\phi}{dt'} = \frac{\partial K}{\partial \delta} = \eta^{(0)}\delta + \eta^{(1)}\delta^2 + \eta^{(2)}\delta^3 \quad , \qquad (12\text{-}1)$$

$$\frac{d\delta}{dt'} = -\frac{\partial K}{\partial \phi} = \lambda\sin\phi \ . \qquad (12\text{-}2)$$

From (12-1) and (12-2), we obtain the fixed points (ϕ, δ) which satisfy the following algebraic equations

$$\eta^{(0)}\delta + \eta^{(1)}\delta^2 + \eta^{(2)}\delta^3 = 0,$$
$$\sin\phi = 0.$$

They are $(0,0), (0, \delta_+), (0, \delta_-), (\pi, 0), (\pi, \delta_+)$, and (π, δ_-) where $\delta_\pm$ are $\dfrac{-\eta^{(1)} \pm \sqrt{\eta^{(1)2} - 4\eta^{(0)}\cdot\eta^{(2)}}}{2\eta^{(2)}}$.

It is trivial to caluculate these values for each cases. The calculated values are shown in Fig.2 and on the figures of each phase space structure. Apparently they agree with the simulation results in the neighbour of the region of interest/3/. This fact means that the Hamiltonian (11) is the correct model of the real system under present considerations.

We have already suspected that the interaction between

different stable resonance regions may lead to a large modification of the RF bucket. The strength of interaction may be described in the term of the distance $L_{\pm}$ between the stable resonace region available for RF rotation and the other stable resonance region, namely

$$L_+ = E_0 |\delta_+| ,$$
$$L_- = E_0 |\delta_-| . \qquad (13)$$

When L_+ is equal to L_-, the effective interaction will disappear, in other words the system approaches a normal pendulum oscillation. It is easy to derive a condition for this; equating L_+ to L_-, we have $\eta^{(1)} = 0$. From this condition, $\alpha^{(1)}$ becomes

$$\alpha^{(1)} = -\frac{3\beta_0^2}{2\gamma_0^2} \simeq -1.667\times10^{-2}. \qquad (14)$$

It is also true that the simulation results, i.e. Fig.1-f gives supprt to the above expectation obtained from the approximate model(11).

2-c $\overline{P}$ Bunch RF Rotation and Effects of Lattice Parameter

In this subsection we show the simulation results of RF rotation. Unfortunately we do not know the value of $\alpha^{(1)}$ which the normal chromaticity correction leaves. Therefore we investigate the system with $\alpha^{(1)}$ which has been chosen in the previous subsection 2-b.

From Table 1, we give one thousand of test particles initial conditions: the full energy spread of 4% (random distribution) and

the full phase spread of 24^{o} (Gaussian with $1\sigma = 4.1^{o}$). Then these test particles are pursued during one quarter rotation in the stationary bucket. To do so, we iterate the recursion equations(1-1),(1-2) for one thousand of initial points which correspond to the above mentioned test particles.

As example, the initial $\overline{P}$ beam and the beam shape which has completed one quarter rotation are shown in Fig.3 and Fig.4. This example is the case with $\alpha^{(1)} = 0$. From the previous subsection , it is easily understood that the modified bucket in Fig.3 and the antisymmetry of bunch tailes in Fig.4 come from the non-linearity for $\Delta P/P_o$.

Now it may be interesting that the rate of the rotated particles which locate within a desired energy spread (0.6%) is represented as the function of $\alpha^{(1)}$. The rate is shown in Fig.5. It, as our expectation, indicates that the RF rotation in the un-modified bucket is most desirable. In addition, Fig.5 has a important meaning on designing a machine. Namely it gives the tolelance on $\alpha^{(1)}$ and its desired standard.

3. Control of Lattice Parameter

3-a Equations for the correction

To make the problem simple, we consider only up to the second order in momentum error $\delta = \Delta P/P_o$, and neglect nonlinear lattice components except for the correcting sextupole magnets. Expanding in the Fourier series, we get the equations as

follows/4/,

for tune shifts,

$$\Delta\nu_i = \nu_{i0}\left(\xi_i^{(0)}\,\delta + \xi_i^{(1)}\,\delta^2\right) \qquad (i = x \text{ or } y) \ ,$$

for the equilibrium orbit in the horizontal oscillation,

$$x_{c.o.d} = \left(\eta_0 + \eta_1\,\delta\right)\delta \ ,$$

and for the circumference,

$$C = C_0\left(1 + \alpha^{(0)}\,\delta + \alpha^{(1)}\,\delta^2\right) \ ,$$

where

$$\xi_i^{(0)} = -\frac{a_{i0}}{2\nu_{i0}^2}$$

$$\xi_i^{(1)} = -\frac{b_{i0} + \nu_{i0}^2\,\xi_i^{(0)2}}{2\nu_{i0}^2} + \frac{1}{4\nu_{i0}^2}\sum_{n>0}\frac{a_{in}^2}{n^2 - 4\left(\nu_{i0}^2 - a_{i0}\delta - b_{i0}\delta^2\right)}$$

$$\alpha^{(0)} = \frac{1}{C_0}\int_0^{C_0}\frac{\eta_0}{\rho}\,ds$$

$$\alpha^{(1)} = \frac{1}{C_0}\int_0^{C_0}\left[\frac{\eta_1}{\rho} + \frac{1}{2}\left(\frac{d\eta_0}{ds}\right)^2\right]ds$$

and

$$\eta_0 = \sqrt{\beta_x}\sum_{m\geq 0}\frac{1}{\nu_{x0}^2 - m^2}\,F_m^0\cos m\phi_x$$

$$\eta_0 + \eta_1 = \sqrt{\beta_x}\sum_{m\geq 0}\frac{1}{\nu_{x0}^2 - m^2}\,F_m^1\cos m\phi_x \ .$$

Fourier components are given by,

$$a_{in} = \pm \frac{1}{2\pi} \int_0^{2\pi} \nu_{i0}^2 \beta_i^2 (g - s\,\eta_0) \cos(n\,\phi_i)\, d\phi_i$$

$$a_{in} + b_{in} = \mp \frac{1}{2\pi} \int_0^{2\pi} \nu_{i0}^2 \beta_i^2 s\,\eta_1 \cos(n\,\phi_i)\, d\phi_i$$

where upper (lower) sign corresponds to x (y) and

$$F_m^0 = \frac{1}{2\pi} \int_0^{2\pi} \frac{\nu_{0x}^2 \beta_x^{3/2}}{\rho} \cos(m\,\phi_x)\, d\phi_x$$

$$F_m^1 = \frac{1}{2\pi} \int_0^{2\pi} \nu_{0x}^2 \beta_x^{3/2} (g\,\eta_0 - \frac{1}{2} s\,\eta_0^2) \cos(m\,\phi_x)\, d\phi_x$$

$$g = \frac{e}{P_0} \frac{\partial B_y}{\partial x} = \frac{1}{(B\rho)_0} \frac{\partial B_y}{\partial x}$$

$$s = \frac{e}{P_0} \frac{\partial^2 B_y}{\partial x^2} = \frac{1}{(B\rho)_0} \frac{\partial^2 B_y}{\partial x^2}$$

$$C = 2\pi R$$

where x and y mean the horizontal and the vertical coordinate, respectively. In the above, we assume that the lattice has a reflection symmetry.

In usual case the main contribution comes from the zero-th harmonic since the lattice elements and the correcting sextupoles are almost uniformly distributed.

First, we assume that the linear chromaticity is already corrected ($\xi_i^{(0)} = 0$) by a usual way, then we can estimate $\xi_i^{(1)}$ and $\alpha^{(1)}$ using the smooth approximation as follows,

$$a_{i0} = -2\,\nu_{i0}^2 (\xi_{i0} + \Delta\xi_i) = 0$$

$$b_{i0} = 2\nu_{i0}^2 \Delta\xi_i - 2F_0'\sqrt{\bar{\beta}_i}\,\Delta\xi_i / \bar{\eta}_0 = -2\nu_{i0}^2 \xi_{i0}(1+\xi_{i0})$$

(assuming $\nu_{x0} = \nu_{y0}$)

$$F_0^0 = \nu_{x0}\sqrt{\bar{\beta}_x} = \sqrt{\nu_{x0}R}$$

$$F_0' = \nu_{x0}\sqrt{\bar{\beta}_x}\,(2\xi_{x0} + \Delta\xi_x) = -\sqrt{\nu_{x0}R}\;\xi_{x0}$$

$$\bar{\eta}_0 = \bar{\beta}_x / \nu_{x0} = R/\nu_{x0}^2$$

$$\xi_i^{(1)} = -b_{i0}/(2\nu_{i0}^2) = \xi_{i0}(1+\xi_{i0})$$

$$\alpha^{(0)} = (F_0^0)^2/(R\nu_{x0}^3) = 1/\nu_{x0}^2$$

$$\alpha^{(1)} = \alpha^{(0)}(-2\xi_{x0} - \Delta\xi_x - 1) = \alpha^{(0)}(-\xi_{x0} - 1) \quad . \qquad (15)$$

In the estimation of $\alpha^{(1)}$, we negrect $d\eta_0/ds$.

Second, we must control $\alpha^{(1)}$ without any change in another parameters. The most perspective way seams to vary the harmonic F_m', $m \tilde{=} \nu_{x0}$ with sextupoles. The contribution from non-zero-th harmonics are given by,

$$\Delta\xi^{(1)} = \frac{1}{4\nu_0^2}\sum_{n>0}\frac{a_n^2}{n^2-4\nu_0^2} + \frac{1}{2\nu_0^2}\sum_{m>0}\frac{F_m' P_m}{\nu_0^2-m^2} \qquad (16)$$

$$\Delta\alpha^{(1)} = \sum_{m>0}\frac{1}{R\nu_0(\nu_0^2-m^2)}F_m^0\Delta F_m' \qquad (17)$$

where $\Delta F_m' = -\frac{1}{4\pi}\int_0^{2\pi}\nu_0^2\,\beta^{3/2}s\,\eta_0^2\cos(m\phi)\,d\phi$

$$P_m = \frac{1}{2\pi}\int_0^{2\pi}\nu_0^2\,\beta^{5/2}s\,\cos(m\phi)\,d\phi \quad .$$

It is enough to consider only the horizontal oscillation because it is easy to keep the changes in the vertical negrigible,

so we do not denote index x from this.

Since the linear lattice elements are almost uniformly distributed, we can neglect terms except for ones caused by sextupoles in Eq.(16) and we get,

$$\Delta\xi^{(1)}=-\frac{1}{\nu_0^2}\left(\frac{\beta}{\eta_0^2}\right)_s\sum_{m>0}\left[\frac{1}{\nu_0^2-m^2}+\frac{1}{4\nu_0^2-m^2}\right](\Delta F'_m)^2 \qquad (16')$$

where index s means values at the location of sextupoles. From Eq.(15) we can roughly approximate $\alpha^{(1)}\cong\alpha^{(0)}$ and the result of the previous section gives the desired value as,

$$\alpha^{(1)}=-\frac{3}{2}\frac{\beta_L^2}{\gamma_L^2} \qquad (\beta_L,\gamma_L : \text{Lorents factors}) .$$

In our problem the maximum momentum error of beam reduces less than 0.5 % after a quarter period of a synchrotron oscillation, so it is reasonable that we impose the condition given by,

$$\nu_0\,|\xi^{(1)}| \le 10^2 .$$

This means that the maximum tune shift is 0.04 at $\delta = \pm 2$ %.

Finally we get the equations for the control of $\alpha^{(1)}$.

$$\Delta\alpha^{(1)}=\sum_{m>0}\frac{F_m^0\,\Delta F'_m}{R\nu_0(\nu_0^2-m^2)} = -\alpha^{(0)}-\frac{3}{2}\frac{\beta_L^2}{\gamma_L^2}$$

$$\nu_0\,|\xi^{(1)}| = \frac{\nu_0^2}{R}\left|\sum_{m>0}\left(\frac{1}{\nu_0^2-m^2}+\frac{1}{4\nu_0^2-m^2}\right)(\Delta F'_m)^2\right| \le 10^2$$

We must remember $a_{i0}=0$ and $\xi_{i0}\cong -1$.

We choose two integers m_1 and m_2 just close to ν_0 and,

$$m_1 < \nu_0 < m_2$$

When we excite $\Delta F'_{m_1}$ and $\Delta F'_{m_2}$ in keeping the ratio $\Delta F'_{m_1}/\Delta F'_{m_2}$

to be about $(\nu_0^2-m_1^2)^{1/2}/(\nu_0^2-m_2^2)^{1/2}$, the variation $\Delta\xi^{(1)}$ is expected to be small enough. We should excite these harmonics in the opposite or the same phase corresponding to the sign of $F^0_{m_1}/F^0_{m_2}$. But if ν_0 is more close to m_1 than m_2, for example, $\Delta\alpha^{(1)}$ is affected mainly by $\Delta F'_{m_1}$, and we only excite $\Delta F'_{m_2}$ according to the ratio mentioned above without any care of the effect on $\Delta\alpha^{(1)}$. We can also expect that β is not affected so much in this control since in the first order we can get,

$$\frac{\Delta\beta}{\beta} = -\delta \sum_{n\geq 0} \frac{2a_n}{4\nu_0^2-n^2} \cos(n\phi) \quad . \tag{18}$$

In principle it is easy to find the best combination of sextupoles. Suppose F and S are vectors composed of the Fourier components to be controlled and of the sextupoler strength, respectively, we can write $F=A\cdot S$. The problem is to find a suitable matrix G which satisfies $F=D\cdot G\cdot S$ where D is diagonal. This gives $G=D^{-1}\cdot A$.

3-b Example

we show the numerical calculations for the proposed debuncher ring of the $\bar{p}$ source/5/. The lattice has a reflection symmetry and the superperiodicity of 2. Its quadrant is shown in Fig.6. Table 3 shows the betatron oscillation parameters at the location of the sextupole magnets. The most effective combination is determined from Table 3 and named mode (a). To compare this with

a bad correction, we also take mode (b). They are shown schematically in Fig.7. Fig.8 ~ 9 show how the parameters vary with the strength of the modulation ΔSF. These parameters are calculated by the program SYNCH. From Fig.10 we summarize as below,

	Mode (a)	Mode (b)	
$\Delta\alpha^{(1)}/\Delta$ SF	-3.8	-7.0	$\times 10^{-2}$ (m^2)
$\nu_0 \Delta\xi^{(1)}/(\Delta SF)^2$	+4.0	-40.	$\times 10^{2}$ (m^4)

In this ring $(\nu_0^2-10^2)^{1/2}/(\nu_0^2-12^2)^{1/2} \cong 1/2$, so $\Delta\xi^{(1)}$ is small as expected in the mode (a). Fig.11 shows the variation of the maximum β in the mode (a). The variation in the first order of momentum error is as small as our expectation with Eq.(18). But the variation in the second and the higher order is so large when $\alpha^{(1)} = -1\times10^{-2}$, since we change η_1 so strongly to get large variation of $\alpha^{(1)}$, and this change excites harmonics a'_n given by,

$$a'_n = -\frac{1}{2\pi}\int_0^{2\pi} \nu_0^2 \beta^2 s \eta_1 \cos(n\phi)\, d\phi$$

Then we can easily get the variation of β in the second oeder in δ as, $\Delta\beta/\beta = -\delta^2 \sum_{n\geq 0} 2a'_n \cos n\phi /(4\nu_0^2 - n^2)$.

In conclusion the control of $\alpha^{(1)}$ in our debuncher ring is limitted by the maximum variation of β in the method mentioned in this section. But it is possible to get $\alpha^{(1)}=0$ which is enough from the results of Section 2, without any trouble in the betatron oscillation.

Figure Captions

Fig.1-a~1-i: The figures show the phase space structure for the system with the parameter $\alpha^{(1)}$ of different values. X or O on each figure mean the unstable, stable fixed point of the approximate system.

Fig.2: Center positions of the stable resonance islands versus the parameter $\alpha^{(1)}$.

Fig.3: The assumed initial shape of the antiproton beam and RF bucket.

Fig.4-a: Bunch shape after 90° RF rotation.

Fig.4-b: Energy distribution after 90° RF rotation.

Fig.5: Momentum reducing efficiency versus the parameter $\alpha^{(1)}$

Fig.6: Quadrant of the debuncher ring.

Fig.7: Excitation modes of the sextupoles.

Fig.8: Variations of the tunes and the momentum compaction parameter in the mode (a).

Fig.9: Variations of the tunes and the momentum compaction parameter in the mode (b).

Fig.10: $\alpha^{(1)}$ and $\xi^{(1)}$ versus the strength of the modulation ΔSF in the mode (a) and (b).

Fig.11: Variations of the maximum values of β in the mode (a).

References and Footnotes

/1/ " TEVATRON I ANTIPROTON SOURCE STATUS REPORT ", FNAL internal report, October (1981).

/2/ K.Takayama, " How we can reduce a momentum spread of 4% in the Debuncher ", FNAL $\bar{P}$-Note 136, July (1981).

/3/ Differences between the real system and model mean that larger terms can not be neglected in such a region.

/4/ H.Wiedemann, " Chromaticity Correction in Large Storage Rings", SLAC PEP-220, September (1976).

/5/ private communication with D.Johnson, Sept. (1981).

Table 3 Betatron Oscillation Parameters at the Sextupoles

SEXTUPOLES							$\beta\eta_0 \cos n\phi$				$\frac{1}{2}\sqrt{\beta_x}\,\eta_0^2 \cos n\phi$				
NAME	STRENG	BX	BY	ETA	PHIX	PHIY	BX20	BX22	BY20	BY22	6	8	10	12	14
		(m)			(deg)										
SD0	0.0000	16.94	9.73	.79	5.90	8.30	-6.26	-8.54	-7.45	-7.67	1.04	.87	.66	.42	.17
SD1	0.0000	4.09	17.50	.88	9.67	16.05	-3.51	-3.04	11.98	15.32	.42	.17	-.09	-.35	-.56
SF1	0.0000	14.60	3.36	2.06	17.67	20.33	29.83	26.31	4.75	.33	-2.23	-6.31	-8.07	-6.85	-3.10
SD2	0.0000	5.26	22.23	1.02	21.25	26.47	2.27	-1.63	-22.37	-16.85	-.73	-1.19	-1.01	-.31	.56
SF2	0.0000	25.30	4.84	1.38	25.27	29.47	-28.82	-33.69	-4.36	2.12	-4.24	-4.47	-1.43	2.64	4.79
SD3	0.0000	3.19	16.08	.58	28.75	35.40	-1.50	.08	9.05	4.81	-.29	-.19	.09	.29	.22
SF3	0.0000	18.71	3.59	.76	36.81	39.73	13.68	.06	.72	-2.46	-.95	.52	1.24	.18	-1.14
SD4	0.0000	6.00	23.19	.56	39.70	45.35	.93	-3.01	-12.90	1.73	-.20	.28	.31	-.17	-.37
SF4	0.0000	20.66	4.52	1.61	43.89	48.40	-30.78	-13.75	-2.73	7.02	-.68	5.81	1.13	-5.73	-1.58
SD5	0.0000	2.67	15.65	1.01	48.27	54.85	-1.13	2.58	15.16	-9.48	.28	.75	-.45	-.65	.60
SF5	0.0000	23.50	3.98	1.99	55.55	58.99	40.16	-36.93	-1.34	-6.27	8.60	.94	-9.28	5.73	5.15
SD6	0.0000	6.25	23.05	.90	58.04	64.20	.89	-5.39	-18.95	18.41	.99	-.25	-.77	.93	-.05
SF6	0.0000	16.10	4.09	1.04	62.85	67.44	-16.67	9.01	-.08	3.06	2.06	-1.72	-.06	1.78	-2.02
SD7	0.0000	2.71	16.35	.48	67.99	74.29	.22	.73	5.46	-7.59	.13	-.19	.14	-.02	-.12
SF7	0.0000	27.47	4.42	.92	74.04	78.07	19.21	-25.06	-2.12	.53	.22	-1.37	2.09	-2.19	1.62

Fig. 1 - a

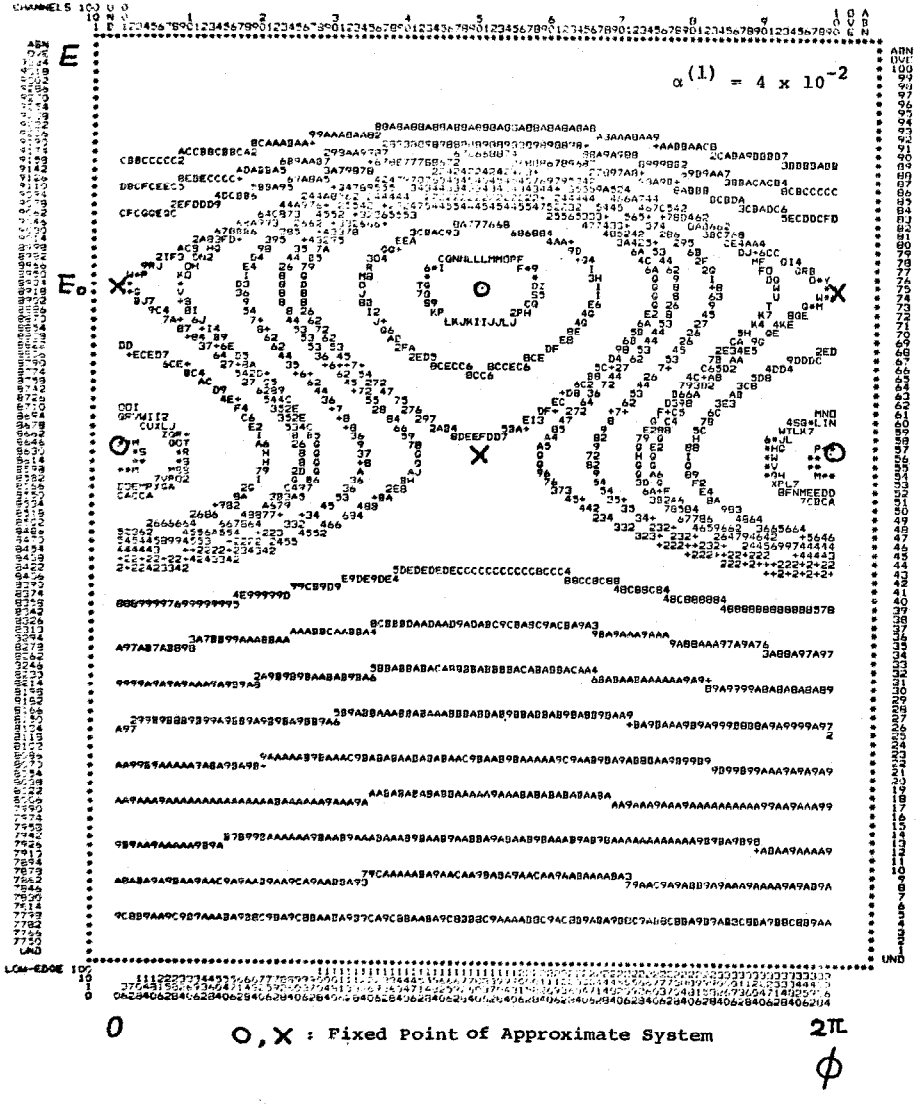

O, X : Fixed Point of Approximate System

Fig. 1 - b

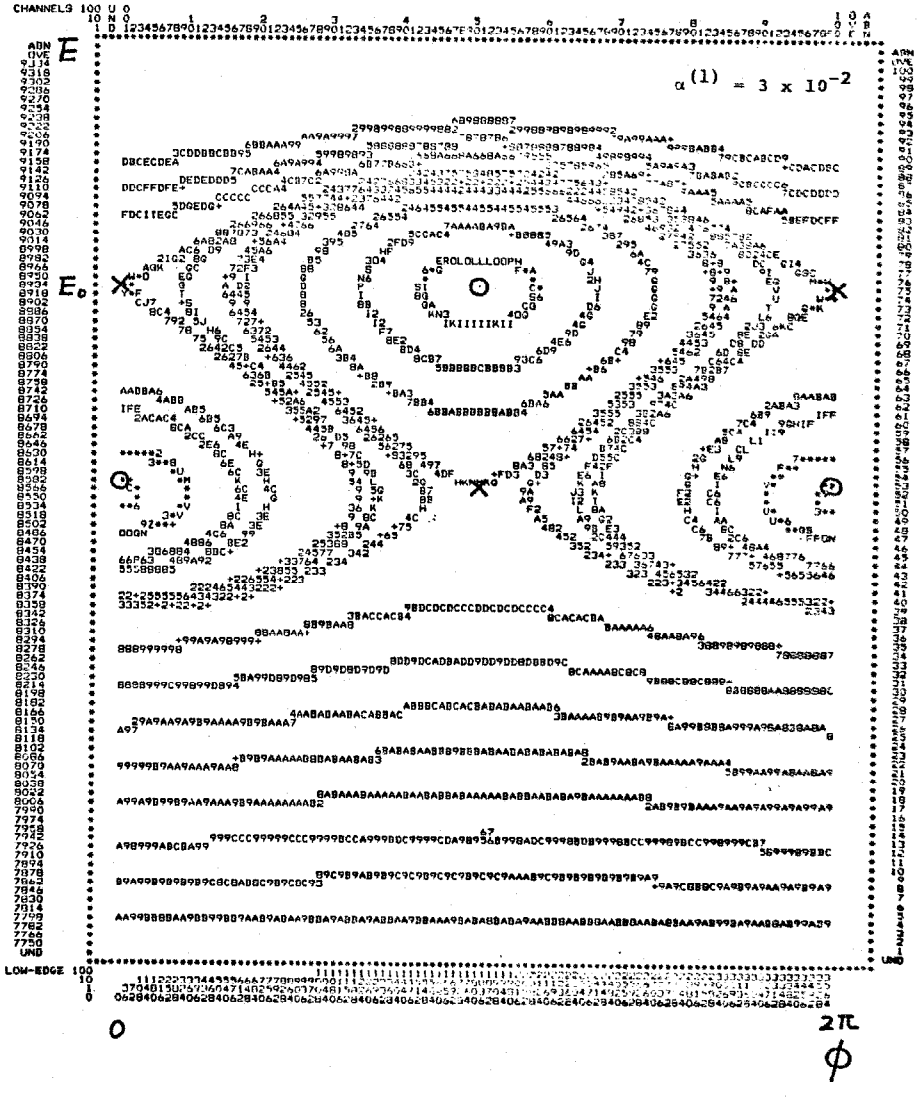

Fig. 1 - c

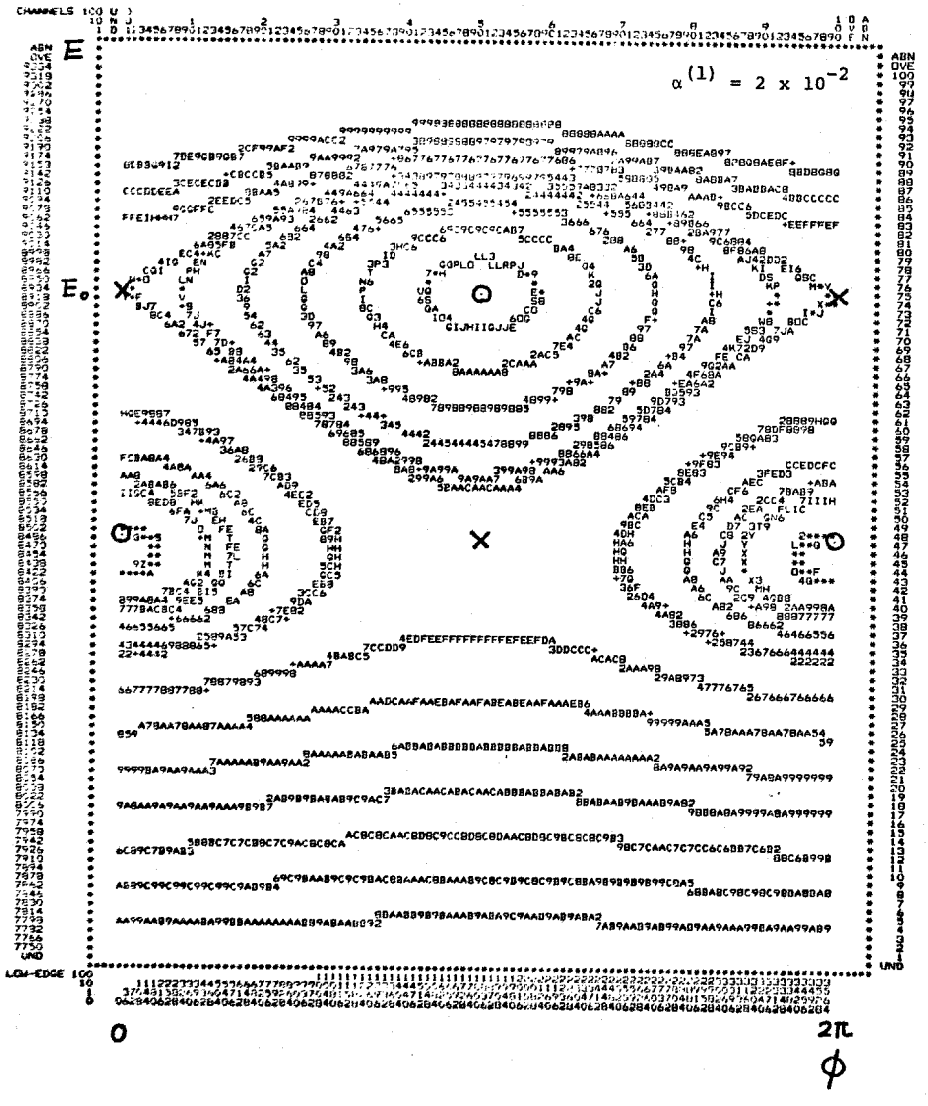

Fig. 1 - d

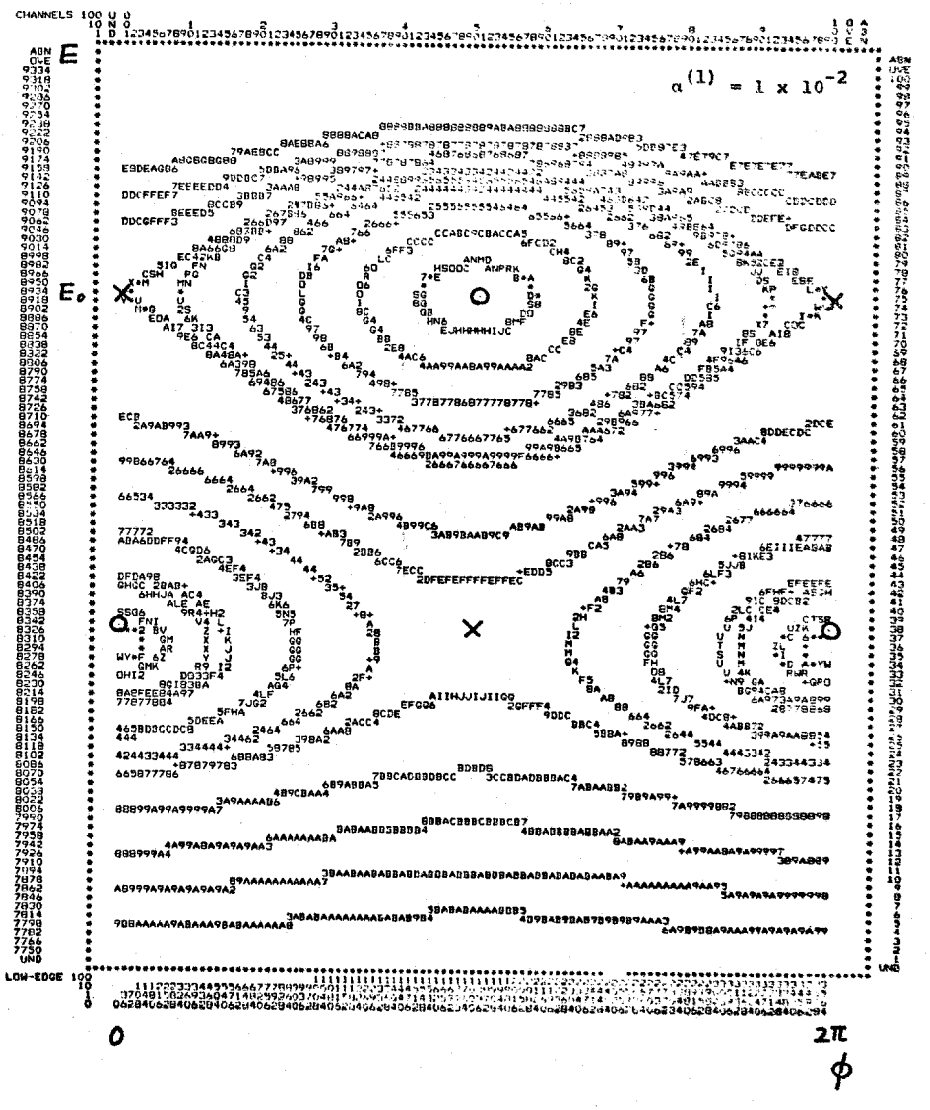

Fig. 1 - e

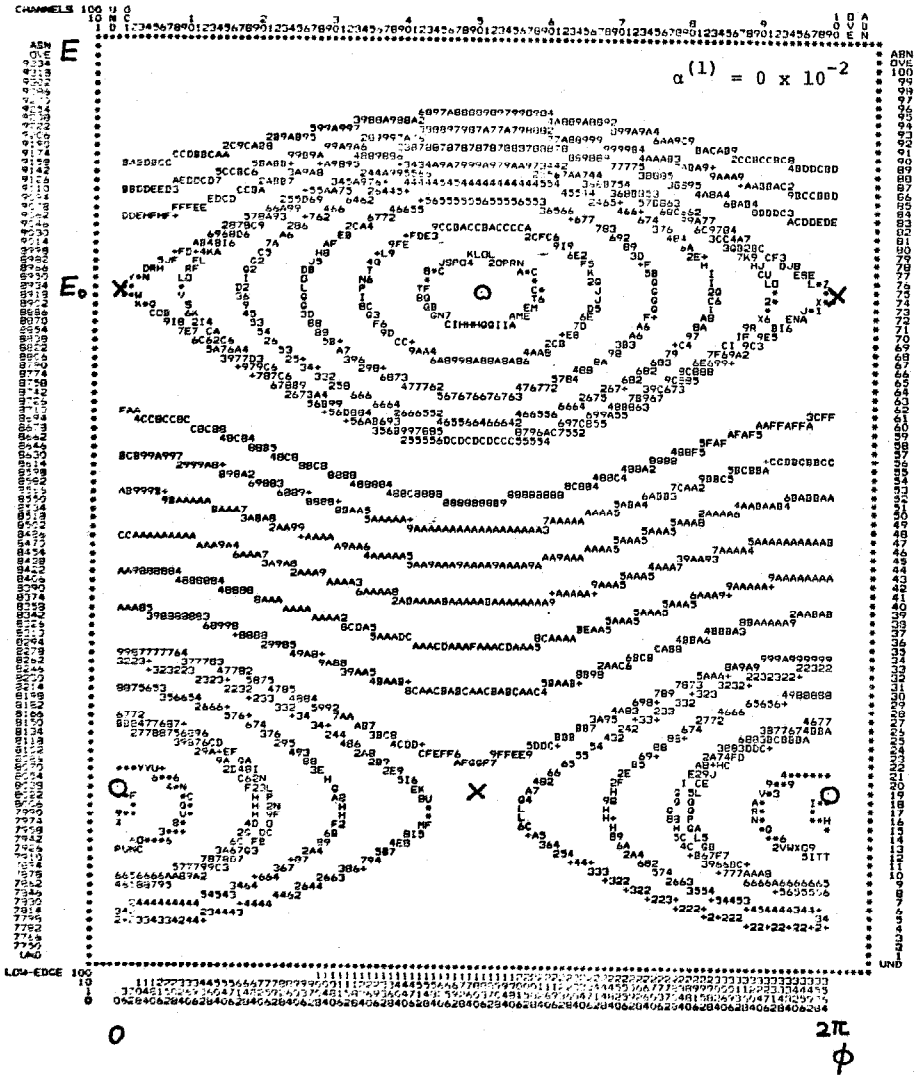
$\alpha^{(1)} = 0 \times 10^{-2}$
E
E_o
0
2π
ϕ

Fig. 1 - f

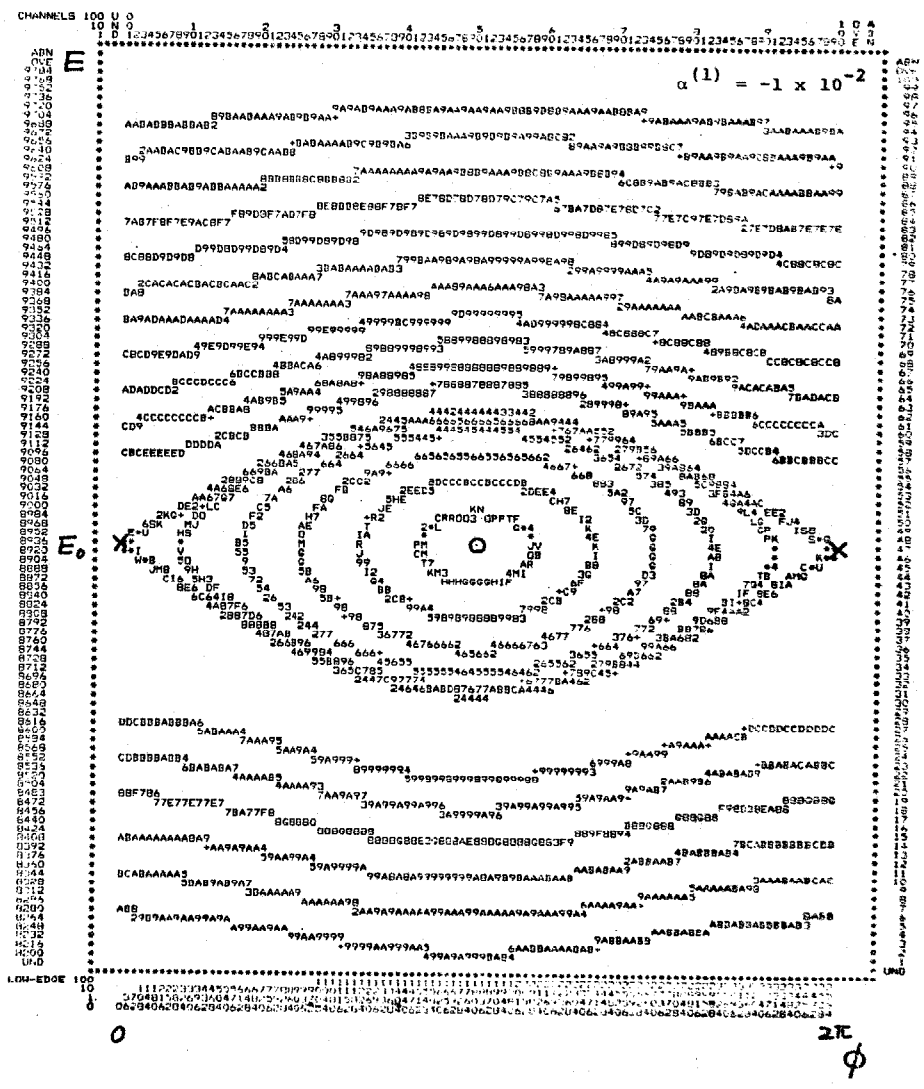
$\alpha^{(1)} = -1 \times 10^{-2}$
E
E_o
0
2π
ϕ

Fig. 1 - g

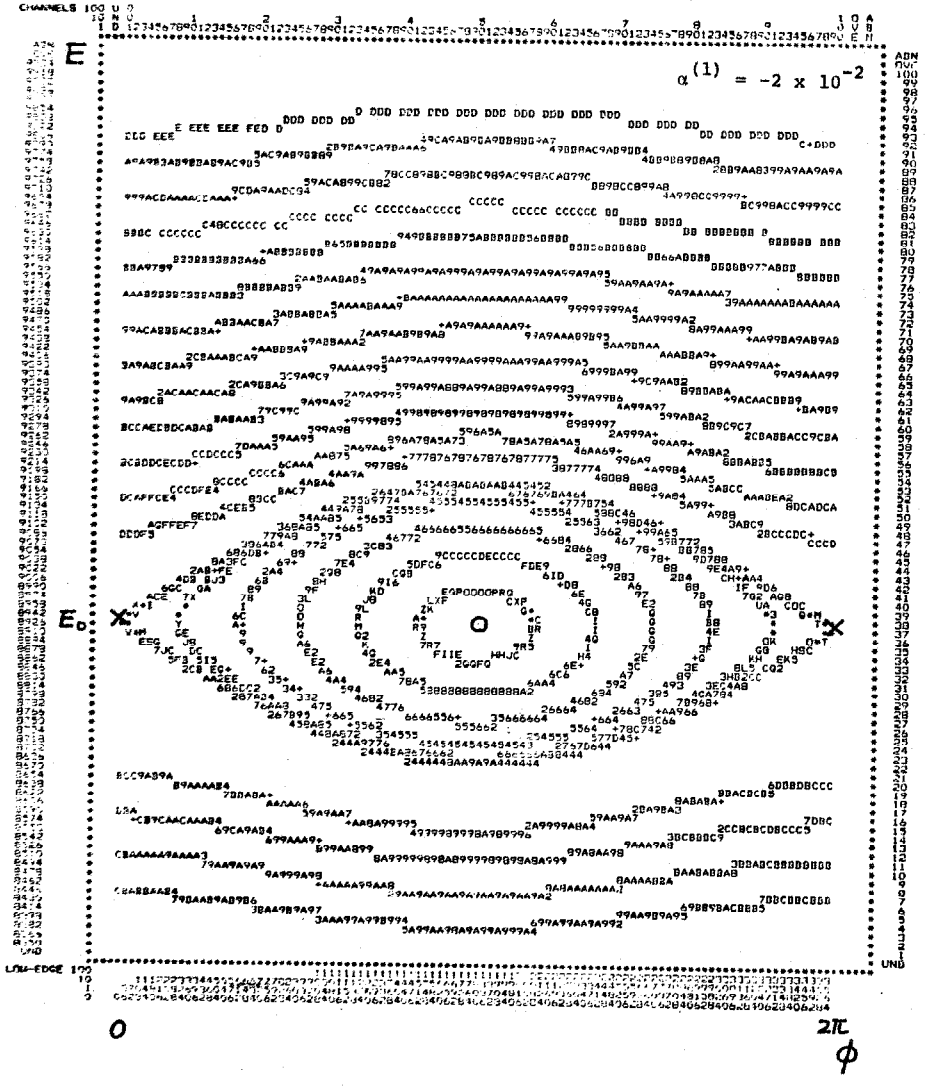
$\alpha^{(1)} = -2 \times 10^{-2}$
E
E_0
0
2π
ϕ

Fig. 1 - h

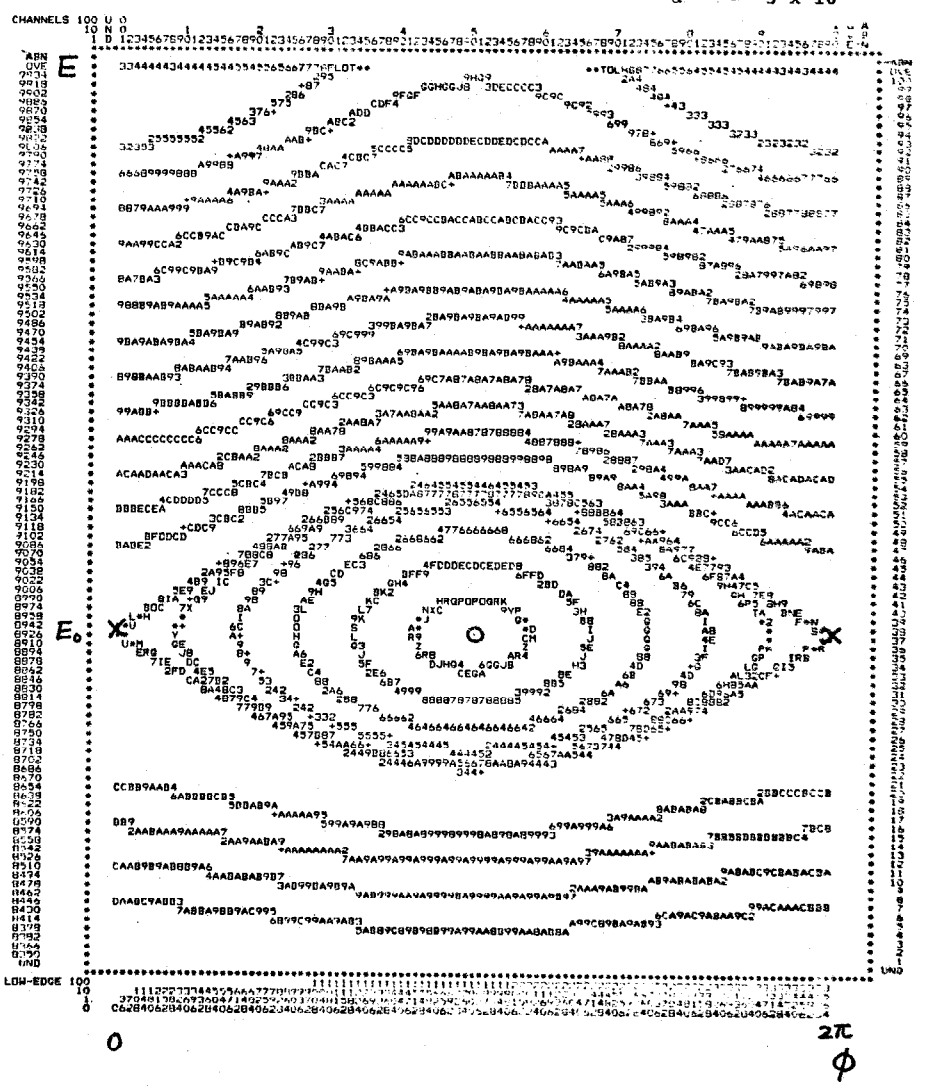
$\alpha^{(1)} = -3 \times 10^{-2}$
E
E_0
0
2π
ϕ

Fig. 1 - i

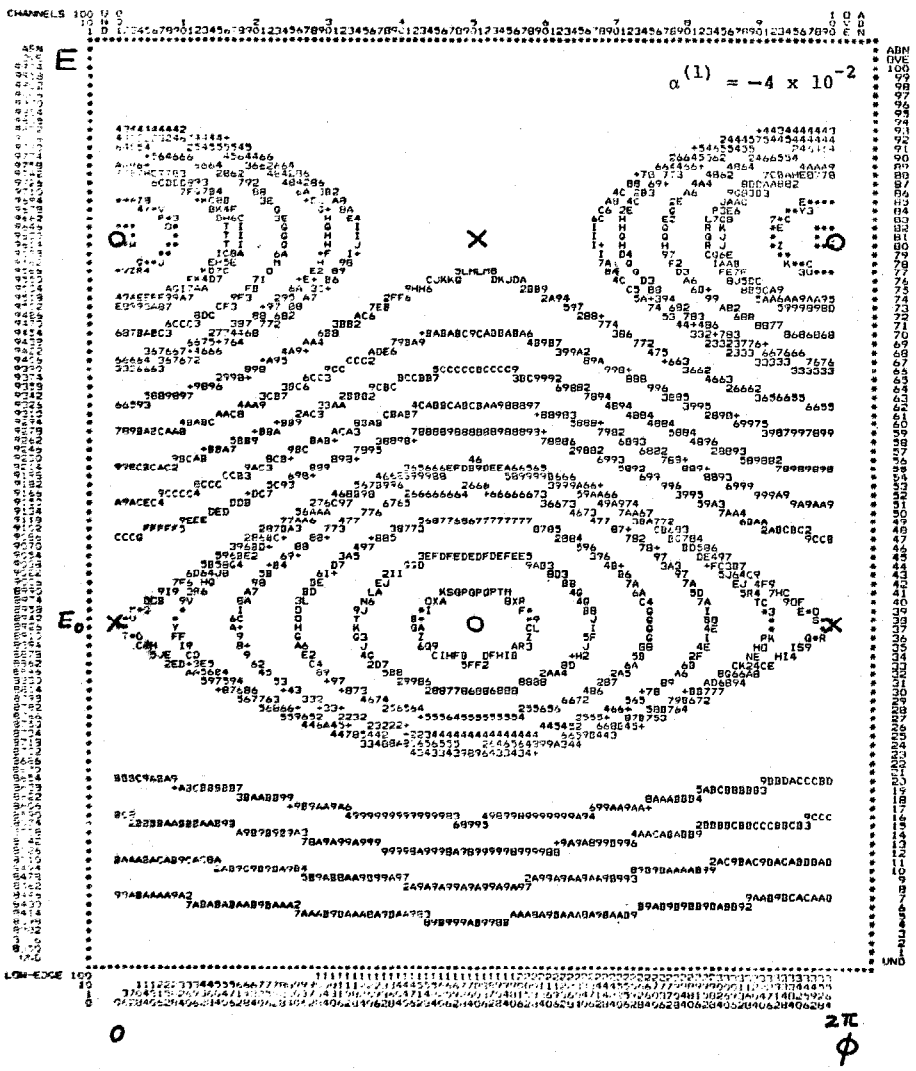
E
E_0
$\alpha^{(1)} = -4 \times 10^{-2}$
0
2π
ϕ

Fig. 2

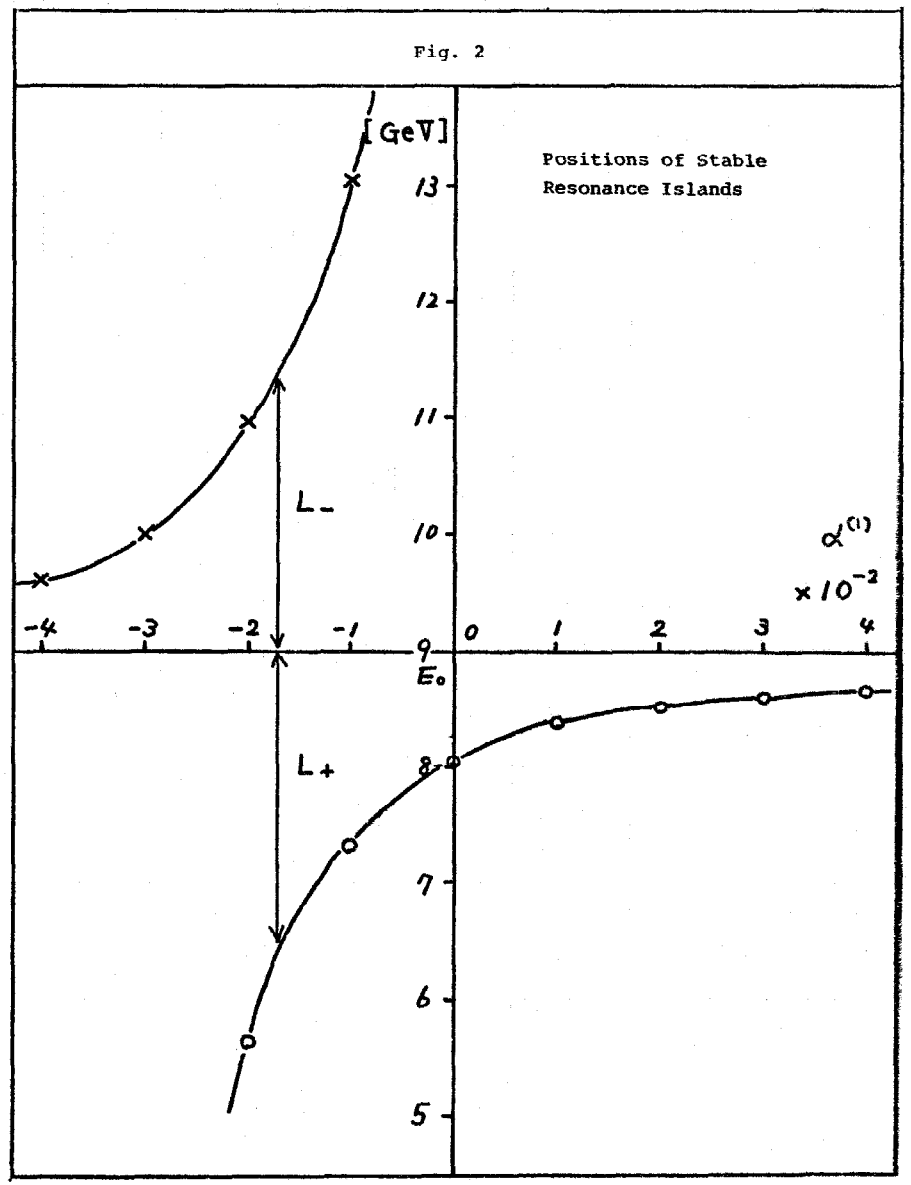
[GeV]
Positions of Stable
Resonance Islands
L-
L+
E_0
$\alpha^{(1)}$
$\times 10^{-2}$
13
12
11
10
9
8
7
6
5
-4
-3
-2
-1
0
1
2
3
4

Fig. 3

Initial Beam Shape and RF Bucket

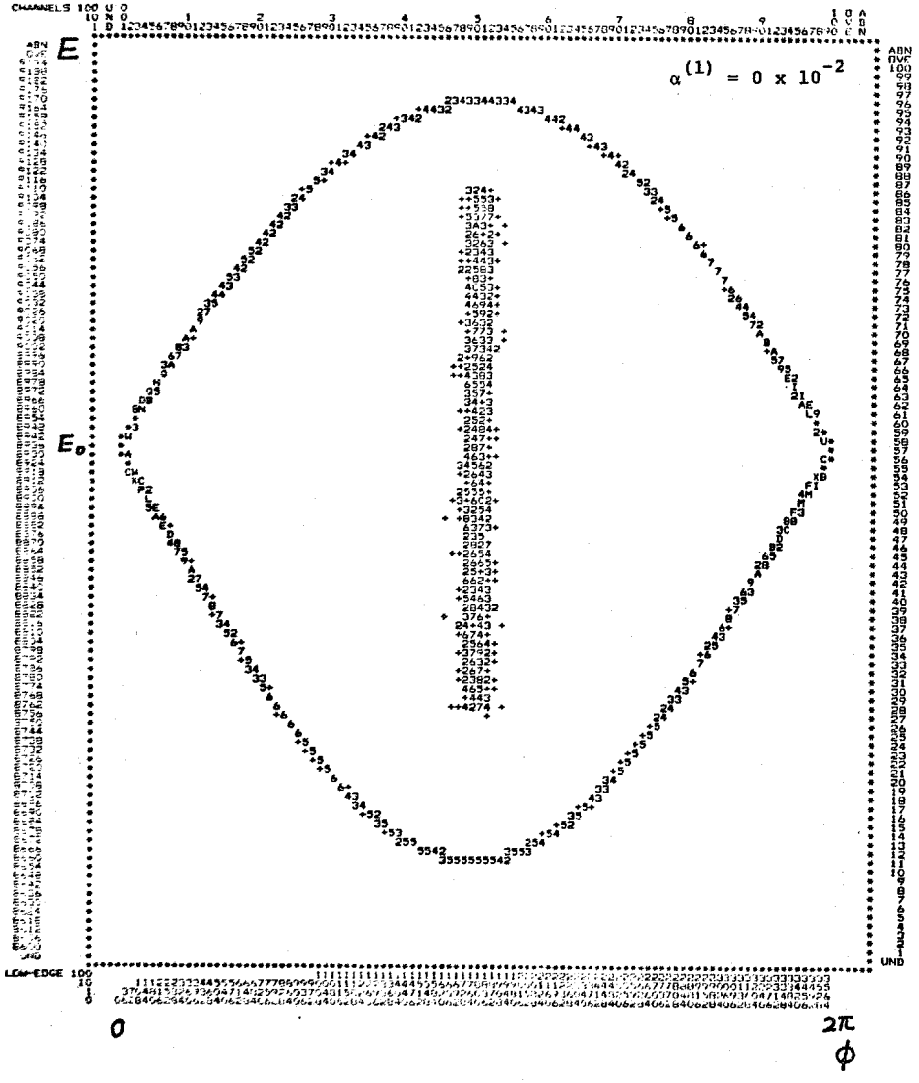

Fig. 4 - a

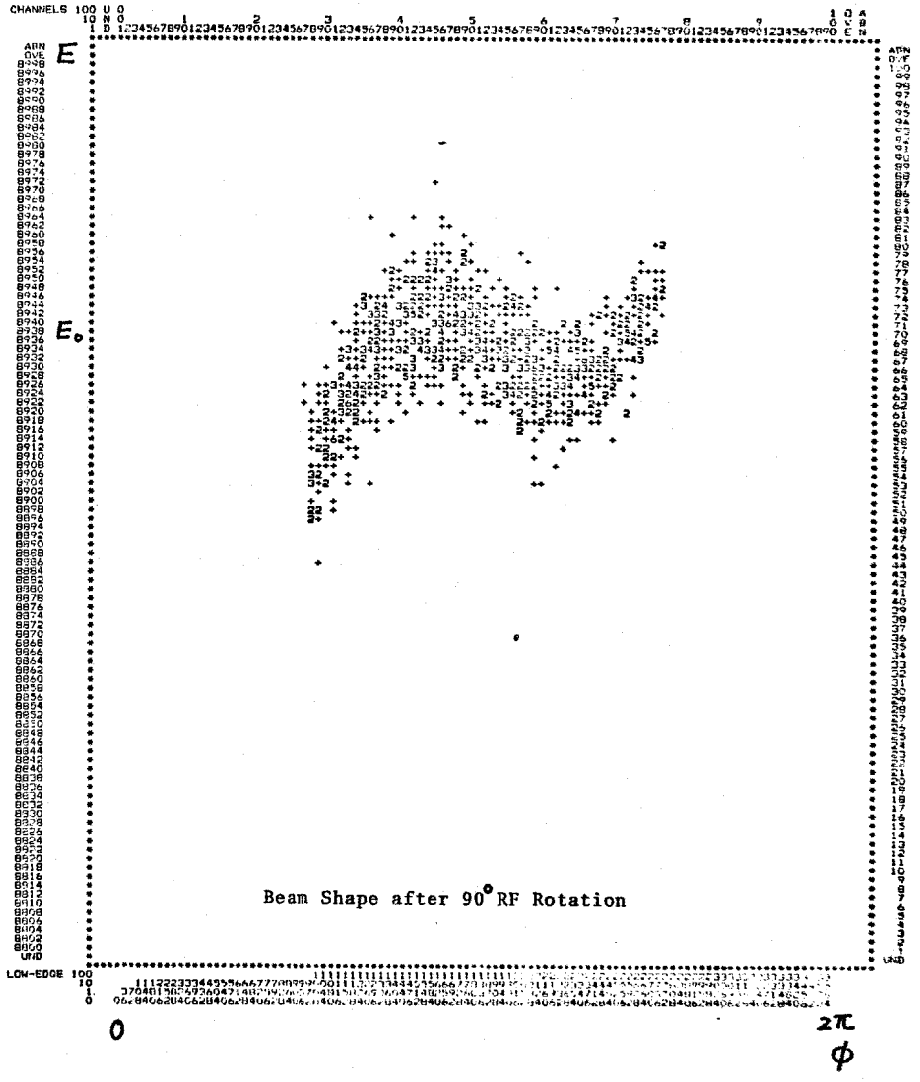

Fig. 4 - b

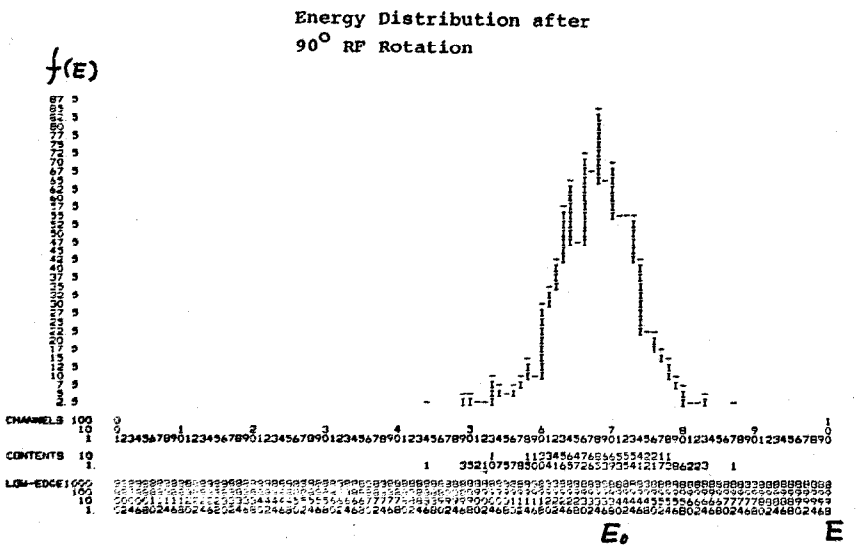
Energy Distribution after
90° RF Rotation
f(E)
CHANNELS
CONTENTS
LOW-EDGE
E₀
E

Fig. 5

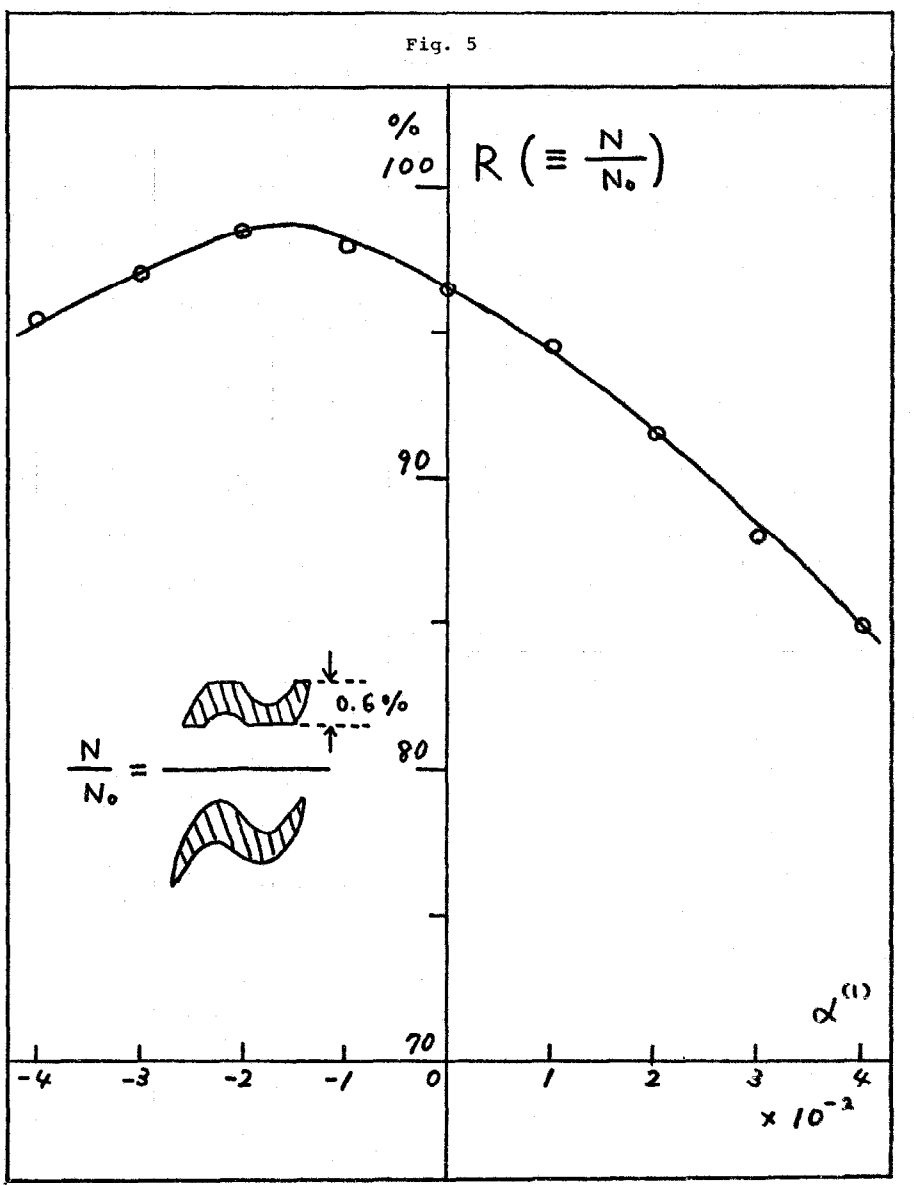
%
100
90
80
70
R (≡ N/N₀)
0.6 %
N/N₀ =
α(1)
-4
-3
-2
-1
0
1
2
3
4
× 10⁻³

Fig. 6 Quadrant of the Debunching Ring

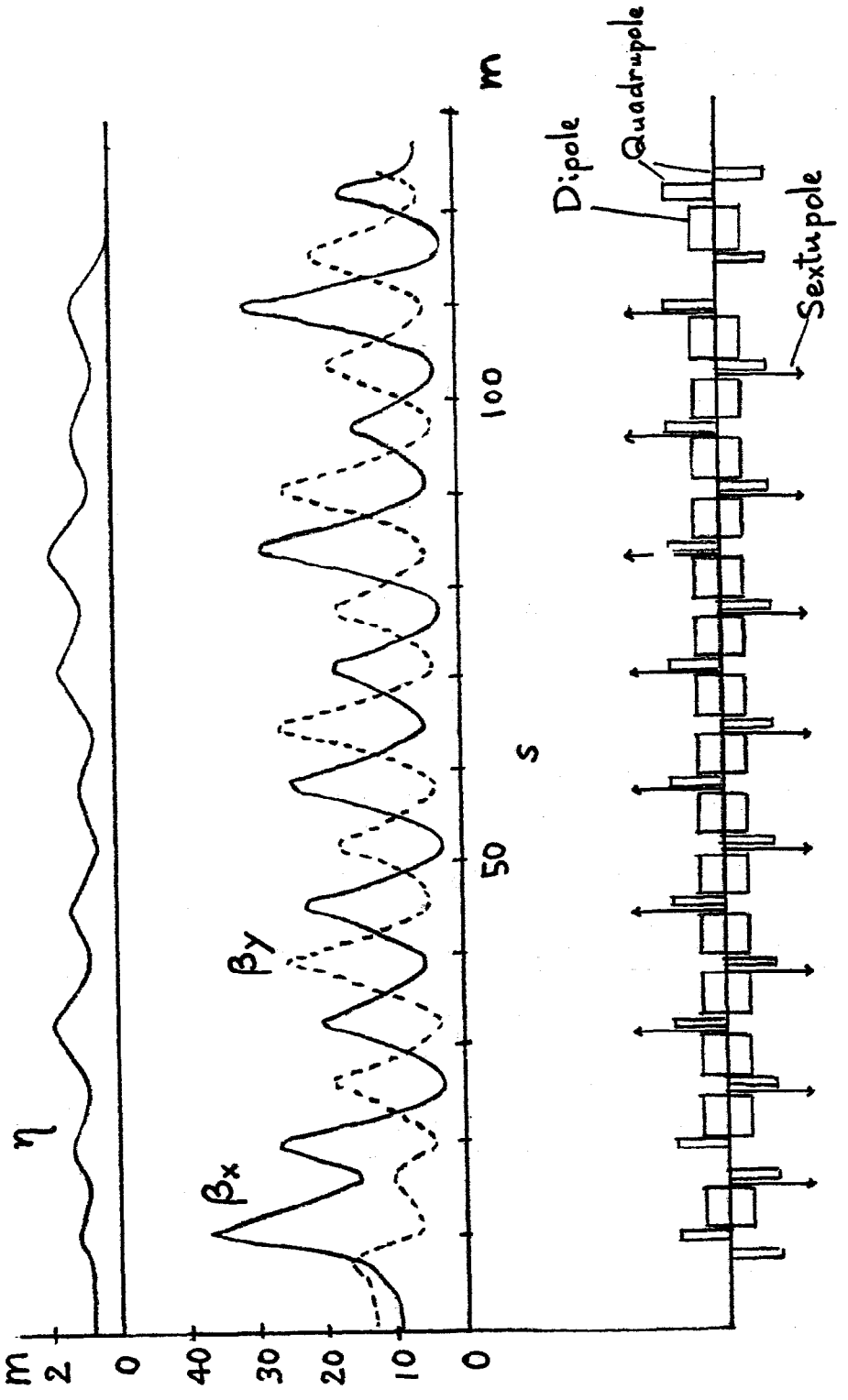

Fig. 7 Excitation Modes of the Sextupoles

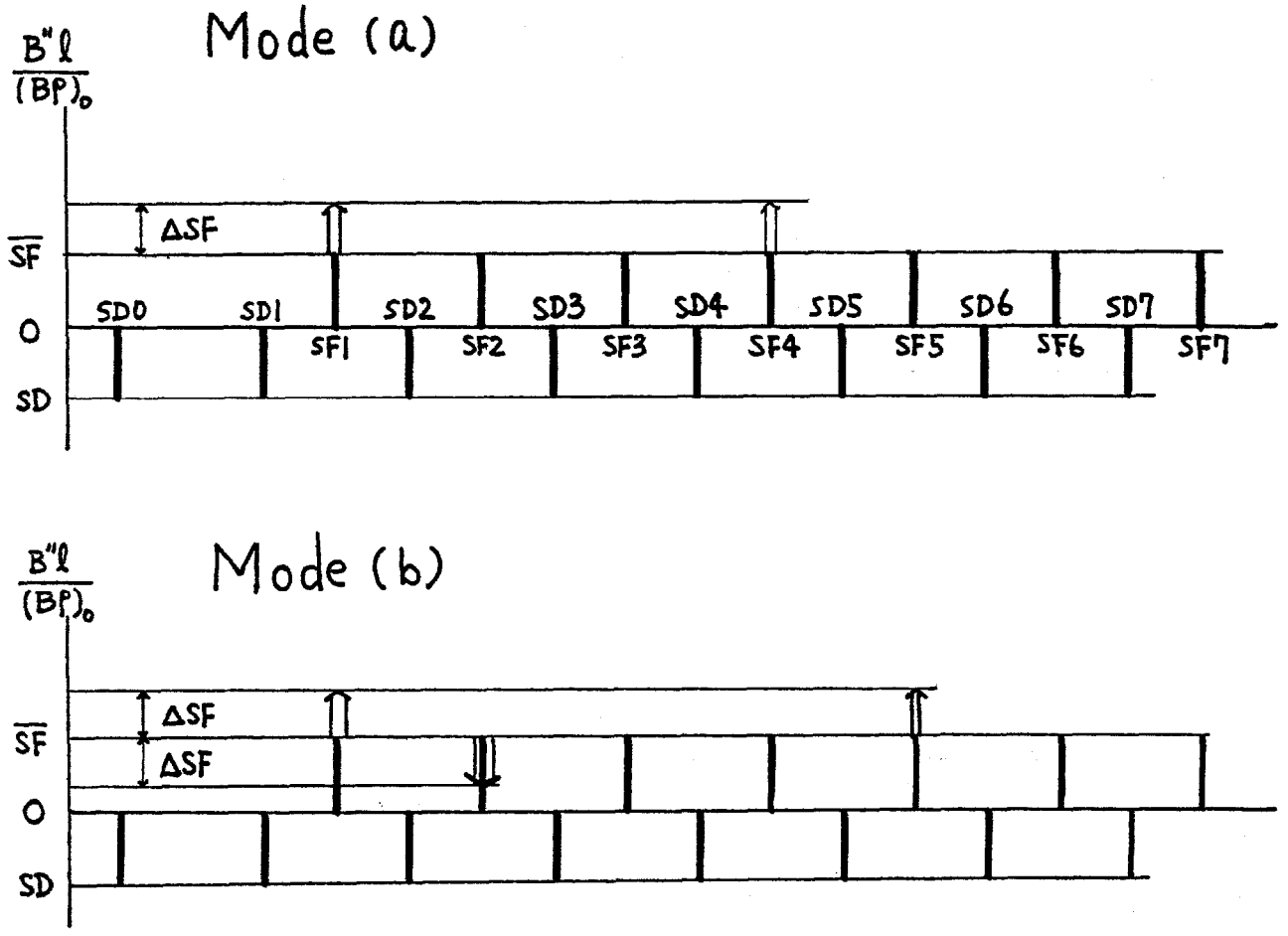

$$\frac{1}{\nu_{x0}\Delta SF}\begin{bmatrix} a_{20} \\ a_{22} \\ \Delta F'_{10} \\ \Delta F'_{12} \end{bmatrix} = \begin{bmatrix} (a) & (b) \\ 0.6 & -63 \\ -8.0 & -15 \\ 4.4 & 10 \\ 8.0 & -2.4 \end{bmatrix} \begin{matrix} \\ \\ m^{1/2} \\ m^{1/2} \end{matrix}$$

Fig. 8 Variations of the tunes and the Momentum Compaction Factor in the Mode (a)

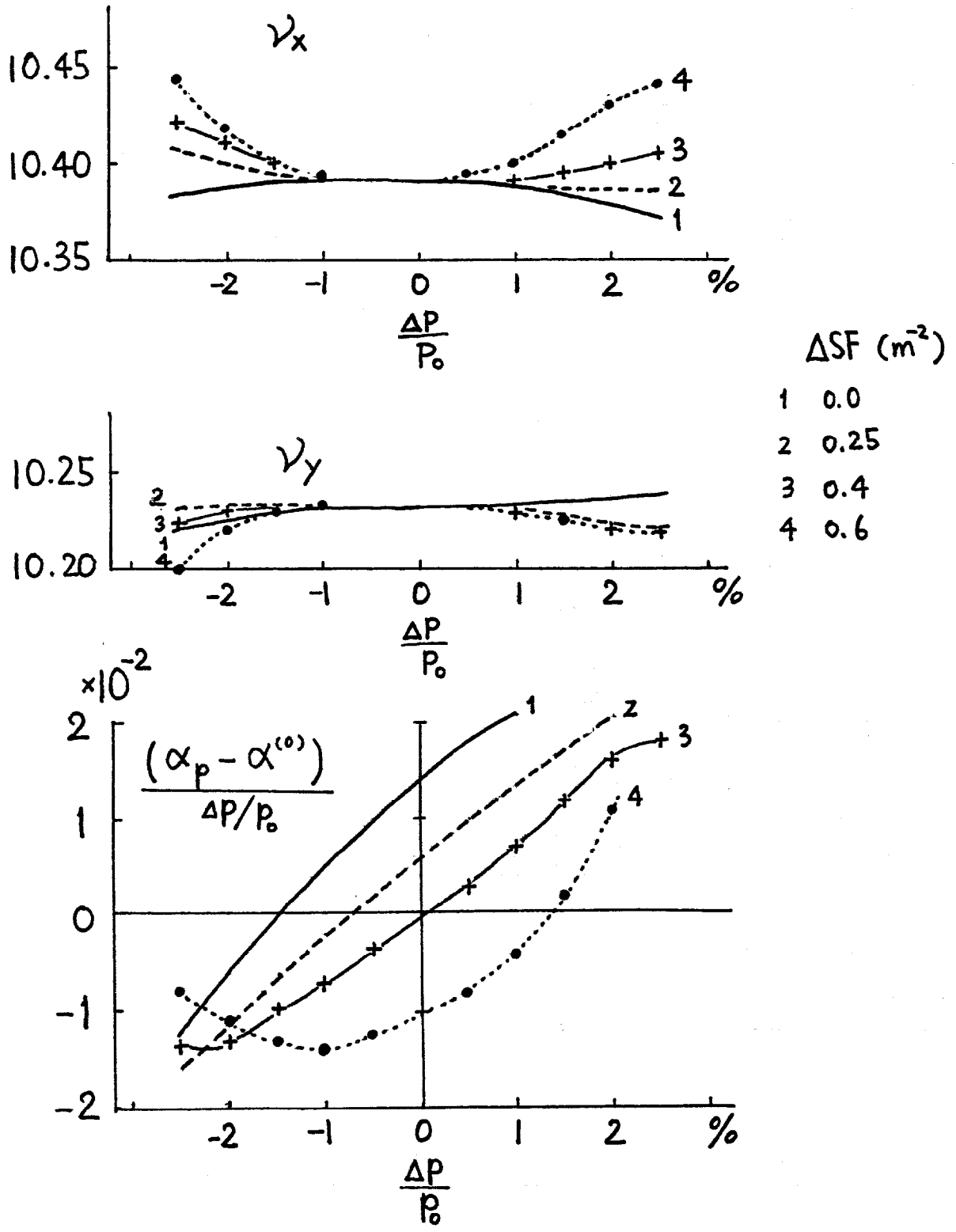

Fig. 9 Variations of the tunes and the Momentum Compaction Factor in the Mode (b)

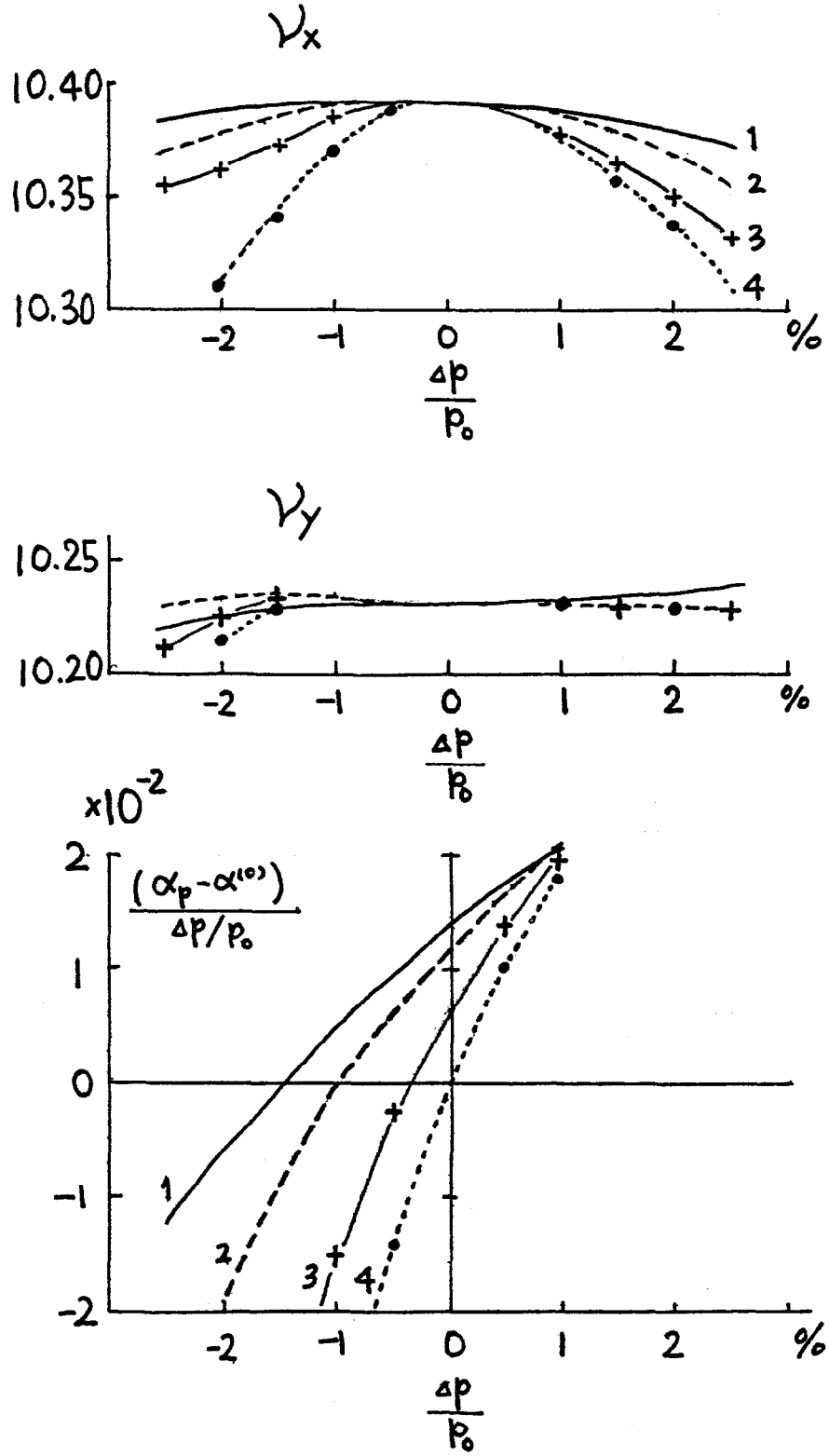

Fig. 10 $\alpha^{(1)}$ and $\xi^{(1)}$ versus the Strength of the Modulation ΔSF in the Mode (a) and (b)

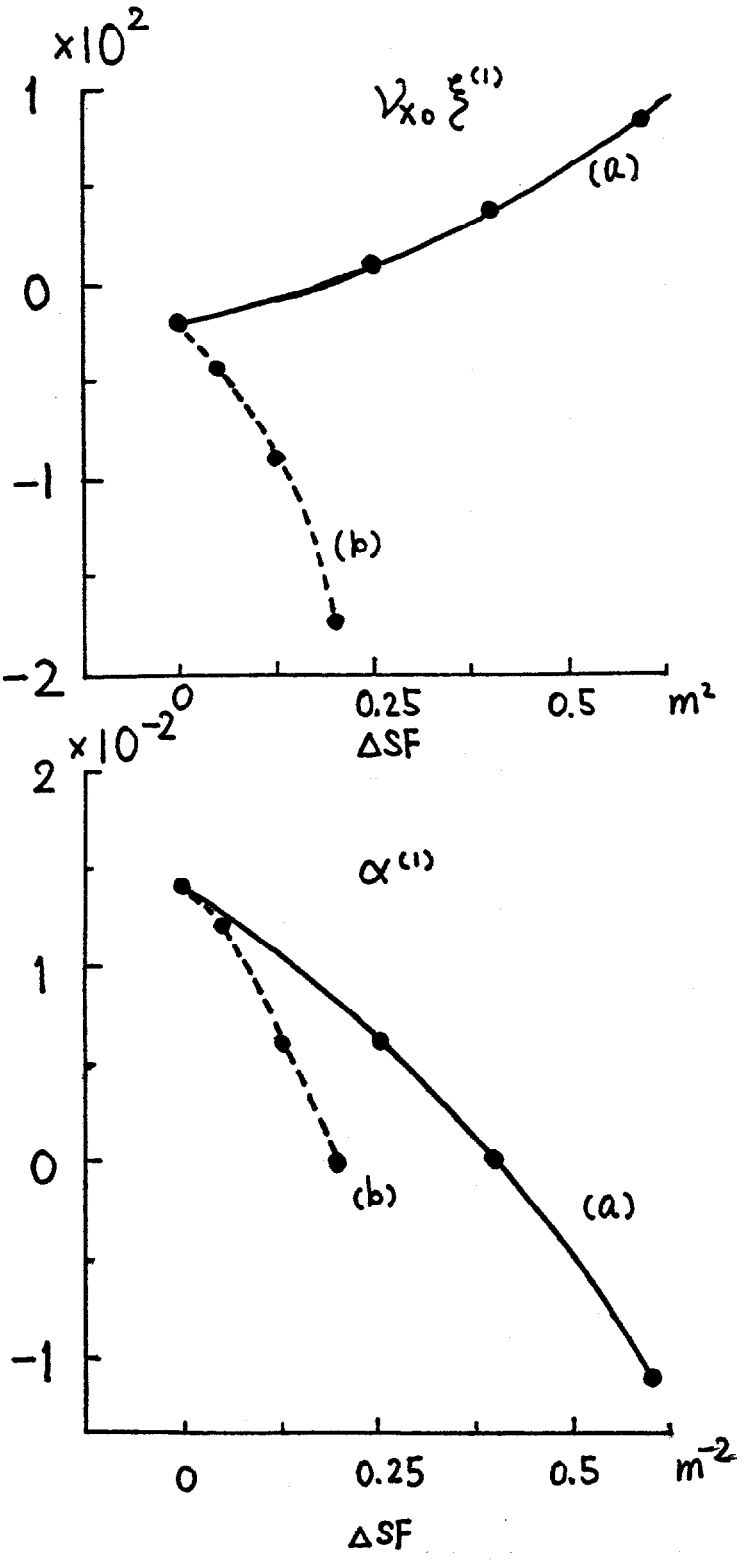

Fig. 11 Variations of the Maximum Values of β in the Mode (a)